Deep-Sea Research Part I 138 (2018) 85–97

Contents lists available at ScienceDirect

Deep-Sea Research Part I

journal homepage: www.elsevier.com/locate/dsri

Micronekton diel migration, community composition and trophic position within two biogeochemical provinces of the South West Indian Ocean: Insight from acoustics and stable isotopes

P. Annasawmy[a,b,*], J.F. Ternon[a], F. Marsac[a,b], Y. Cherel[c], N. Béhagle[d], G. Roudaut[d], A. Lebourges-Dhaussy[d], H. Demarcq[a], C.L. Moloney[b], S. Jaquemet[e], F. Ménard[f]

[a] Institut de Recherche pour le Développement (IRD), UMR 248 MARBEC (IRD/IFREMER/UM2/CNRS), Avenue Jean Monnet, CS 30171, 34203 Sète cedex, France
[b] Department of Biological Sciences and Marine Research Institute, University of Cape Town, Private Bag X3, Rondebosch 7701, Cape Town, South Africa
[c] Centre d'Etudes Biologiques de Chizé, UMR7372 du CNRS-Université de la Rochelle, 79360 Villiers-en-bois, France
[d] Institut de Recherche pour le Développement (IRD), UMR LEMAR 195 (UBO/CNRS/IRD), Campus Ifremer, BP 70, 29280 Plouzané, France
[e] Université de La Réunion, UMR ENTROPIE (UR/IRD/CNRS), Avenue René Cassin CS92003, 97744 Saint-Denis Cedex 9, France
[f] Aix Marseille Univ, Université de Toulon, CNRS, IRD, MIO, Marseille, France

ARTICLE INFO

Keywords:
Micronekton
Diel vertical migration
Indian South Subtropical Gyre
East African Coastal province
Trophic level

ABSTRACT

Spatial distribution, community composition and trophic roles of micronekton (crustaceans, fishes and squids) were investigated in the Indian South Subtropical Gyre (ISSG) province and the East African Coastal province (EAFR), by combining acoustic surveys, mid-water trawls and stable isotope analyses from scientific cruises conducted in 2009 and 2010. Mesopelagic micronekton performed diel vertical migrations in both provinces, from deep (400–740 m) to surface (0–200 m) layers at dusk and in the opposite direction at dawn, with some species migrating below 740 m. The EAFR province was more dynamic than the oligotrophic ISSG province, with enhanced eddy activity and enhanced yearly productivity. The active enrichment mechanisms in the EAFR, in terms of available primary production, led to high micronekton acoustic density (as a proxy of micronekton abundance) and large micronekton weight and abundance estimates from trawl data. Particulate organic matter in the EAFR exhibited greater enrichment in ^{13}C and ^{15}N compared to the ISSG and, consequently, tissues of selected micronekton organisms in the EAFR were more enriched in ^{15}N (higher $\delta^{15}N$ values). In both provinces, micronekton encompassed a wide range of isotopic niches, with large overlaps between species. Micronekton and swordfish in the EAFR had an overlapping range of $\delta^{15}N$ values, contrasting with the ISSG province where swordfish were two trophic levels higher than the sampled micronekton. Our results provide some evidence that the combined action of riverine input and the dynamics of eddies might influence productivity in the EAFR, and hence the abundance of micronekton and the enrichment of tissues in ^{15}N, compared to the oligotrophic ISSG province.

1. Introduction

Mesopelagic micronekton typically range in size from 2 to 20 cm. They can be divided into broad taxonomic groups such as crustaceans, fishes, squids (Brodeur and Yamamura, 2005; De Forest and Drazen, 2009) and gelatinous organisms. Most mesopelagic micronekton perform extensive diel vertical migrations (DVM), from deep layers to surface layers (upper 200 m) at dusk and from surface to deep layers (below 400 m) at dawn (Lebourges-Dhaussy et al., 2000; Béhagle et al., 2014). Migrant micronekton are thought to acquire organic material at the ocean surface (Longhurst, 1990; Hidaka et al., 2001). Part of the assimilated material is released during the day as respiratory carbon and excretory nitrogen as micronekton migrate towards deeper layers (Bianchi et al., 2013; Catul et al., 2011; Hidaka et al., 2001). Vertically migrating organisms are thus key components in transferring energy and essential minerals and nutrients between epipelagic primary and secondary production to deeper regions of the world's oceans via respiration, excretion and natural mortality (Hidaka et al., 2001; De Forest and Drazen, 2009; Ariza et al., 2015). They also contribute in the energy transfer to higher trophic levels, since micronekton are

* Corresponding author at: Institut de Recherche pour le Développement (IRD), UMR 248 MARBEC (IRD/IFREMER/UM2/CNRS), Avenue Jean Monnet, CS 30171, 34203 Sète cedex, France.
E-mail address: angelee-pavanee.annasawmy@ird.fr (P. Annasawmy).

https://doi.org/10.1016/j.dsr.2018.07.002
Received 14 June 2017; Received in revised form 22 June 2018; Accepted 2 July 2018
Available online 03 July 2018
0967-0637/

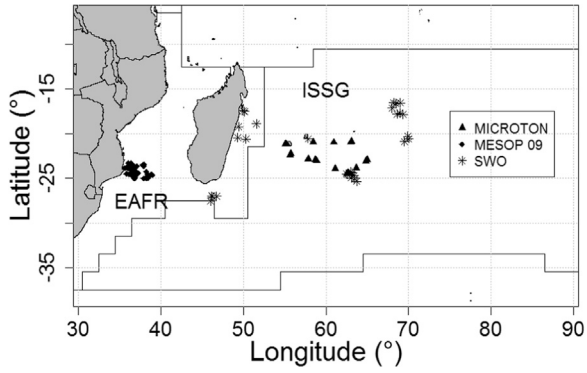

Fig. 1. Map of the MICROTON CTD stations (triangle symbols) in the Indian South Subtropical Gyre (ISSG) province, of the MESOP 2009 CTD stations (diamond symbols) in the East African Coastal province (EAFR) and sites of swordfish sampling (SWO, star symbols). Longhurst's (2007) biogeochemical provinces (ISSG and EAFR) are delimited by black solid lines.

intensively preyed upon by various top predators such as tunas, swordfish and seabirds (Guinet et al., 1996; Bertrand et al., 2002; Potier et al., 2007; Cherel et al., 2010; Danckwerts et al., 2014; Jaquemet et al., 2014).

In the global ocean, large predatory fishes such as yellowfin-, albacore- and bigeye tunas and swordfish are distributed across distinct biogeochemical provinces with contrasting environmental conditions in terms of sea surface temperature (SST), mean chlorophyll *a* concentrations, salinity, stratification of the water column and thermocline depth (Reygondeau et al., 2012). Although habitat cues affect movements of top predators, their abundance, spatial distribution and species composition are mostly driven by the presence of foraging species, which are closely linked to environmental factors (Lehodey et al., 1998; Beaugrand et al., 2002).

The main objective of this study was to investigate micronekton dynamics (diel migration, community composition and trophic relationships) in two major biogeochemical provinces of the South West Indian Ocean: the Indian South Subtropical Gyre (ISSG) and the East African Coastal Province (EAFR). The ISSG ranges between latitudes 10°S and 40°S (Fig. 1). It is characterised by a large-scale anticyclonic gyre (Stramma and Lutjeharms, 1997; Longhurst, 2007; Pous et al., 2014) and is considered to be oligotrophic (Jena et al., 2013; Sutton et al., 2017). The EAFR extends from 5°S to Cape Agulhas (Fig. 1) and is characterised by the presence of mesoscale cyclonic and anticyclonic eddies propagating southwards through the Mozambique Channel (Schouten et al., 2003; Quartly and Srokosz, 2004). These eddies are known to enhance oceanic production in low and high trophic levels in the Mozambique Channel (Lamont et al., 2014; Lebourges-Dhaussy et al., 2014; Béhagle et al., 2014; Potier et al., 2014; Jaquemet et al., 2014). Considering the contrasting environmental patterns between the ISSG and EAFR provinces, we hypothesize that the dynamics of micronekton communities must differ significantly between these two provinces.

To test our hypotheses, we used acoustic surveys to investigate the large-scale distribution and DVM patterns of micronekton, trawl surveys to assess the micronekton community composition and stable isotope analyses to determine the trophic relationships between predators and prey, the trophic level of selected micronekton organisms and the source of carbon and energy exploited by micronekton. Stable nitrogen isotope ($\delta^{15}N$) values have been shown to increase in a predictable manner between consumers and their primary prey items (with an enrichment of 2–4‰ in $\delta^{15}N$ values at each trophic step), thereby reflecting the trophic position of the consumer (Vanderklift and Ponsard, 2003; Michener and Kaufman, 2007; Martínez Del Rio et al., 2009). Differences in stable carbon isotope ($\delta^{13}C$) values indicate sources of primary production, such as inshore versus offshore, or pelagic versus benthic contributions to food intake (Hobson et al., 1994; Rubenstein and Hobson, 2004).

2. Material and methods

2.1. Study area and scientific cruises

The MICROTON cruise (DOI: ⟨http://dx.doi.org/10.17600/10110010⟩) took place in the ISSG province on board the *R/V ANTEA*. Samples and data (Table 1) were collected from 19 March to 5 April 2010 between latitudes 21°00S and 24°30'S, and longitudes 55°00–64°50'E (Fig. 1). The MESOP 2009 cruise (DOI: ⟨http://dx.doi.org/10.17600/9110050⟩) took place in the EAFR province on board the *R/V ANTEA*. Samples and data were collected from 27 October to

Table 1
Summary of the data collected and analyses carried out during MICROTON in the ISSG and MESOP 2009 in the EAFR.

Province/Cruises	Variable	Characteristics	MICROTON (ISSG)	MESOP 2009 (EAFR)
Satellite	MSLA	1/4° resolution	Daily at the dates corresponding to CTD or trawl stations	Daily at the dates corresponding to CTD or trawl stations
	SSC and SST	MODIS, 4.5 km resolution	Daily to produce five-day composites over the period of the cruise	Daily to produce five-day composites over the period of the cruise
Acoustic	s_A	38 kHz frequency	Continuous along transect lines	Continuous along transect lines
Oceanography	CTD with fluorometer	0–1000 m Temperature, dissolved oxygen, fluorescence Nitrate estimations	25 stations	54 stations
Biological	POM	5 m (POM-Surf) and at the fluorescence maximum (Fmax), 4–8 L' filtration, Stable isotope analyses	POM-Surf: 14 samples POM-Fmax: 14 samples	POM-Surf: 29 samples POM-Fmax: 26 samples
	Zooplankton	Bongo net 200 and 300 µm, 0–200 m	Day: 3 tows Night: 15 tows 0–200 m Stable isotope analyses	No stable isotope analyses
	Micronekton	40 m IYGBP trawl, 80 mm front, 5 mm cod end mesh Stable isotope analyses	Day: 2 trawls 0–200 m 4 trawls below 400 m 1 trawl 200–400 m Night: 10 shallow trawls 2 deep trawls	Day: 5 trawls 0–200 m 2 trawls 200–400 m Night: 12 shallow trawls 1 deep trawl
	Swordfish	Pelagic longline catch Stable isotope analyses	172 tissue samples	96 tissue samples

23 November 2009 between latitudes 23°00S and 26°00S and longitudes 35°00–39°00E (Fig. 1).

Swordfish dorsal muscle samples (Table 1; Fig. 1) were collected from fish caught by pelagic longline during additional cruises carried out in the ISSG from 21 September to 20 October 2009, and in the EAFR province in October and November 2009 on board the catamaran BRAHMA during the IOSSS ESPADON project (https://wwz.ifremer.fr/lareunion/Projets/Grands-pelagiques/IOSSS-ESPADON).

2.2. Satellite monitoring of the oceanic environment

Delayed-time mean sea level anomalies (MSLAs) at a daily and 1/4° resolution, produced and distributed by the Copernicus Marine Environment Monitoring Service project (CMEMS) and available at http://marine.copernicus.eu/, were used to describe the mesoscale eddy field during both MICROTON (ISSG) and MESOP 2009 (EAFR). Values of the SLA (cm) and geostrophic velocity anomaly (cm s^{-1}) corresponding to each CTD or trawl station (see Section 2.4) were interpolated from the altimetry products at the dates and locations of the stations. Eddy kinetic energy (EKE) was calculated from altimetry geostrophic current anomalies using the equation:

$$EKE\ (cm^2\ s^{-2}) = (u^2 + v^2) \quad (1)$$

where u and v represent the zonal and meridional components of the surface geostrophic current anomaly (cm s^{-1}). Each hydrographic station was categorized according to its location in a cyclonic or anticyclonic eddy, or a frontal-, divergence- or shelf region, based on a discriminant functional analysis using sea level anomaly, geostrophic current speed and high resolution bathymetry (e.g. Lamont et al., 2014).

We used sea surface chlorophyll (SSC) data from the MODIS sensor (http://oceancolor.gsfc.nasa.gov), with a daily and 4.5 km resolution, to calculate 5-day averages that were used as a proxy of surface oceanic primary production. Monthly mean chlorophyll *a* concentrations for the defined regions (ISSG: 18–27°S/53–67°E; EAFR Coast: 20–30°S/30–36°E; EAFR Mozambique Channel: 20–30°S/36–40°E) were averaged from September 2009 to August 2010. Five-day averages of MODIS SST were produced from the same source and at the same spatial resolution as the SSC ocean color product. The VGPM "chlorophyll-based" model using the standard algorithm from Behrenfeld (2009), was used to estimate net primary production for November 2009 and March 2010.

2.3. Acoustic surveys

Acoustic data were collected continuously (day and night) with a Simrad EK60 echosounder working at four frequencies (38, 70, 120 and 200 kHz) and at a cruising speed of 8–9 knots for maximum noise reduction. The pulse duration was set to 0.512 ms and the transmitted power to 1000 W. The water column was accurately sampled to a depth of 740 m during data acquisition using the 38 kHz frequency. Below this depth, acoustic data were of poor quality owing to the bad weather conditions during the cruises. The acoustic data were processed using the Movies + software (Ifremer) to remove background noise, white pings and echo parasites that might have appeared because of high wind stress and swells during parts of the cruises. An offset of 10 m below the sea surface was applied to account for acoustic interference from surface turbulence. The along-track sampling unit was 1 nautical mile (nmi). Echo-integration was performed at an Sv threshold of − 80 dB and on 20-m layers except for the first layer, which started at 10 m below the sea surface (10–20 m).

The micronekton acoustic density was determined by the nautical area scattering coefficient (NASC, s_A, m^2 nmi^{-2}, related to the backscattered energy), which can be used as a proxy of the relative biomass of micronekton, provided certain assumptions are met (Béhagle et al., 2014). Diurnal and nocturnal periods were processed separately to assess diel variation. Crepuscular periods (dawn and dusk), which correspond to transition periods of micronekton ascent and descent, were excluded from the analyses through visual screening of the echograms (e.g. Béhagle et al., 2014). The water column was separated into three depth categories: 10–200 m (surface layer), 200–400 m (intermediate layer) and 400–740 m (deep layer), following an initial analysis of the echograms, which indicated that organisms were organised vertically into three main layers. Only the 38 kHz data were used for further statistical analyses because they had the greatest vertical range of the frequencies common to all of our surveys. To characterize DVM of micronekton, the depths were calculated at which 50% and 75% of the total s_A value were found in the water column (integrated from the sea surface to 740 m).

2.4. In situ measurements, sample collection and laboratory analyses

CTD casts (MICROTON: 25 stations; MESOP 2009: 54 stations), were conducted to profile temperature, salinity, dissolved oxygen and fluorescence of the water column from the surface to 1000 m using a Seabird 911 Plus CTD equipped with a Wetlabs ECO FL fluorometer. In the absence of a precise fluorometer calibration, fluorometry data are expressed in relative units. CTD fluorometry profiles indicated the exact depth of the deep chlorophyll maximum (DCM). The average depths of the thermocline were assessed from the CTD profiles using the 20 °C isotherm depth as a proxy. Sea water from Niskin bottles was sampled for chlorophyll *a* and nutrient measurements at the surface (0–10 m) and at the DCM. Samples collected for nutrient measurements were pasteurised at 80 °C, stored at room temperature on board and later analysed by standard auto-analyser techniques (Oudot et al., 1998) in Brest (France) for nitrate concentrations. Chlorophyll *a* filters were stored in aluminium foil and frozen on board at − 80 °C before being subjected to high-performance liquid chromatography in the laboratory (Brest, France) to measure chlorophyll *a* concentrations.

Particulate organic matter (POM) was collected for stable isotope analyses from Niskin bottles at 5 m (referred to as POM-Surf) and at the depth of maximum fluorescence (referred to as POM-Fmax). Suspended POM particles were obtained by filtering 4–8 L (depending on the load of each sample) of seawater on precombusted 25 or 47 mm glass-fibre filters (0.7 µm mesh size). After filtration, the filters were oven-dried at 50 °C for 24 h and saved at room temperature in aluminium foil before being processed to determine C and N stable isotope ratios using mass spectrometry (see Section 2.5).

Zooplankton samples in the ISSG province were collected at night (3 tows) and during the day (15 tows) in the top 200 m of the water column using a 200 and 300 µm mesh size bongo net towed at a speed of 2 knots for 30–45 min (flow rate of approximately 3.1 m^3 s^{-1}). The samples were frozen on board at − 20 °C. In the laboratory, defrosted samples from the 300 µm sieve were sorted into two main groups (copepods and mysids), which were the most abundant taxa in the nets. Stable isotope analyses were performed on copepods and mysids from MICROTON only (see Section 2.5). Stable isotope analyses were not carried out on MESOP 2009 zooplankton samples.

Micronekton organisms were collected with a 40-m long International Young Gadoid Pelagic Trawl, with an 80-mm knotless nylon delta mesh netting in the front tapering to 5 mm at the codend. It was towed at a speed of 3–4 knots for 30 min. Night tows were carried out in the shallow layer (0–200 m) in the ISSG (n = 10) and the EAFR (n = 12) and in the deep layer (450–590 m) in the ISSG (n = 2) and the EAFR (n = 1). Day tows were carried out on micronekton aggregations detected by acoustics in the shallow layer in the ISSG (n = 2) and the EAFR (n = 5), in the deep layer in the ISSG (n = 4), and in the intermediate layer (200–400 m) in the ISSG (n = 1) and the EAFR (n = 2). The micronekton organisms were sorted on board and broadly divided into four categories: gelatinous organisms, crustaceans, fishes and squids. The wet weights of the four broad categories were measured.

The micronekton components were counted and identified on board to the lowest possible taxon. Approximately 2–5 mg of soft tissues (dorsal muscle for fishes, abdomen muscle for crustaceans, mantles for squids) of some individuals (selected according to their occurrence and abundance) and whole leptocephali larvae and salps were sampled on board for stable isotope analyses (see Section 2.5).

2.5. Stable isotope analysis

Zooplankton, micronekton and swordfish samples to be analysed for stable isotopes were freeze-dried with the Christ Alpha 1-4 LSC Freeze Dryer for 48 h, before being ground to a fine homogeneous powder using the automatic ball mill RETSCH MM200. Dichloromethane was used on an accelerated solvent extraction system (ASE®, Dionex; Bodin et al., 2009) to remove lipids. Prior to $\delta^{13}C$ analyses, POM filters and zooplankton samples were reacted with 2 N HCl to remove carbonates. Untreated sub-samples of POM and zooplankton were used to measure $\delta^{15}N$ since acid treatment may lead to the loss of nitrogenous compounds. All samples were sent to La Rochelle University (LIENSS, UMR 7266 CNRS) for stable isotope analysis by an EA-IRMS (isotopic ratio mass spectrometry coupled to an elemental analyser). The samples were subjected to combustion in the elemental analyser to separate CO_2 and N_2 gases. A reference gas set was used to determine isotopic ratios by comparison. The isotopic ratios are expressed as parts per thousand (‰) and using the conventional δ notation (Supplementary information, Table 1).

The trophic level (TL) of each specimen was calculated using the equation proposed by Minagawa and Wada (1984) with the reference level set at a trophic level of 2 for the primary consumer:

$$\text{Trophic level} = 2.0 + \frac{\delta^{15}N_i - \delta^{15}N_{primary\ consumer}}{3.2} \quad (2)$$

where $\delta^{15}N_i$ is the nitrogen isotopic composition of any given micronekton taxon i, $\delta^{15}N_{primary\ consumer}$ is the $\delta^{15}N$ reference baseline value at trophic level 2, and 3.2‰ is an estimate of the trophic enrichment factor between consumers and their primary prey (Martínez Del Rio et al., 2009; Cherel et al., 2010; Ménard et al., 2014).

Primary consumers, POM or zooplankton can be used as isotopic baselines in TL estimates (Lorrain et al., 2015). In order to reduce errors, primary consumers are generally used as the baseline (Martínez Del Rio et al., 2009). Pyrosomes are known phytoplankton filter feeders and were thus chosen for estimating TLs for samples from both cruises. The $\delta^{15}N$ reference baseline value (Eq. (2)) used for MICROTON (ISSG) samples was the mean of 5.0 ± 1.1‰ derived from ten *Pyrosomatida*, and for MESOP 2009 (EAFR) samples it was the mean of 5.2 ± 0.8‰ derived from four *Pyrosomatida*.

An analysis of variance (ANOVA) in R version (3.3.1) was performed to test differences among the different micronekton feeding modes (filter feeder, detritivore, omnivore and carnivore) in terms of their $\delta^{15}N$ and $\delta^{13}C$ values. Information on individual micronekton feeding habits was obtained from the literature. The gelatinous organisms, *Salpa maxima* and *Pyrosomatida*, were classified as filter feeders (von Harbou, 2009), but Siphonophora were classified as carnivores (Mapstone, 2014). Leptocephali larvae were classified as detritivores (Otake et al., 1990). Crustaceans were classified as omnivores since they were reported to feed on zooplankton, euphausiids and copepods, and are also known for occasional herbivory (Tanaka et al., 2007), except for *Nematobrachion sexspinosum*, which was reported to have a carnivorous feeding mode (Hu, 1978). The majority of mesopelagic fishes were classified as carnivores because they feed on copepods, amphipods, euphausiids and ostracods (Pakhomov et al., 1996; Hudson et al., 2014; Bernal et al., 2015; Young et al., 2015). The fish species *Ceratoscopelus warmingii* was classified as an omnivore since it was reported to feed on zooplankton and is also known for occasional herbivory (Robison, 1984). Squids were classified as carnivores, being reported to prey upon copepods, amphipods, euphausiids, larvae and fries of carnivorous fishes (Arkhipkin et al., 1998), and on lanternfishes for larger-sized specimens (Young et al., 2015) (Supplementary information, Table 1).

2.6. Data viewing and statistical analyses

Matlab routines were used to extract the SLA, surface geostrophic current and EKE for the date and location of each station sampled and to plot the SLA distribution for MICROTON (ISSG) and MESOP 2009 (EAFR).

The differences between day and night acoustic density estimates (s_A) across all thirty-seven depth bins ($L_{10–20}$, $L_{20–40}$, $L_{40–60}$,…, $L_{720–740}$) for both cruises were investigated using pairwise Wilcoxon rank sum tests, Kruskal-Wallis tests and post-hoc procedures. All values are given as mean ± S.D.

A canonical correspondence analysis (CCA, Oksanen et al., 2017) was carried out using R (version 3.3.1) routines to identify patterns in the distribution of micronekton species across stations, constrained by the environmental variables SSC, SST, minimum oxygen concentrations (MinOxy), SLA, depths of the thermocline (Thermocline.Depth) and DCM (DCM.Depth), and minimum oxygen layer (MinOxy.Depth). The result is represented as a two-dimensional graph, with the environmental variables plotted as centred vectors. The magnitude of variation of each environmental variable is proportional to the length of the vector, the direction of which indicates increasing values of the variable.

Links between $\delta^{15}N$ and/or $\delta^{13}C$ values and the broad micronekton categories were investigated using MANOVA, Kruskal-Wallis tests and pairwise comparisons. Isotopic niches were determined using the stable isotope bayesian ellipses in R (SIBER, Jackson et al., 2011). The trophic niche widths (standard ellipse corrected area, SEA_c, calculated using Bayesian inference) of each group (POM-Surf, POM-Fmax, zooplankton-during MICROTON only-, gelatinous organisms, crustaceans, squids, mesopelagic fishes and swordfish) were described in terms of the space that the group occupies on a $\delta^{15}N$-$\delta^{13}C$ plot based on all the individuals within the group.

A linear model was applied using R to test for the effect of the three environmental variables (chlorophyll *a*, temperature and nitrate) on $\delta^{13}C$ and $\delta^{15}N$ of POM collected during MICROTON (ISSG) and MESOP 2009 (EAFR). Linear models were also applied in R to investigate the influence of body length on $\delta^{15}N$ values of all micronekton broad categories and swordfish in the ISSG and in the EAFR, and the influence of body length on $\delta^{15}N$ values of *Ceratoscopelus warmingii*, *Vinciguerria nimbaria*, *Diaphus richardsoni*, *Hygophum hygomii*, *Funchalia* spp., and *Sthenoteuthis oualaniensis*, selected because of their common occurrence in both provinces, large sample sizes and wide body-length ranges.

3. Results

3.1. Oceanographic conditions in the study regions

The sampled region in the ISSG was mainly dominated by anticyclonic eddies of moderate amplitude, whereas in the EAFR a combination of intense cyclonic and anticyclonic eddies was recorded (Fig. 2A). The mean EKE calculated from altimetry data for all the sampled stations was five times greater in the EAFR (1036 ± 875 cm^2 s^{-2}) than the ISSG (188 ± 109 cm^2 s^{-2}).

Based on in situ CTD data, the mean surface chlorophyll *a* value recorded across all ISSG stations was lower (0.03 ± 0.01 mg m^{-3}) than that recorded in the EAFR (0.18 ± 0.09 mg m^{-3}). In the ISSG, the mean chlorophyll *a* values derived from satellite SSC over the area (18–27°S/53–67°E) increased from 0.06 ± 0.005 mg m^{-3} in March–April 2010 to a maximum of 0.13 mg m^{-3} in August 2010 (Fig. 2B). The March–April MICROTON observations took place during an increasing phase of oceanic productivity. In the EAFR, the mean satellite-derived chlorophyll *a* in December 2009 decreased to a minimum concentration

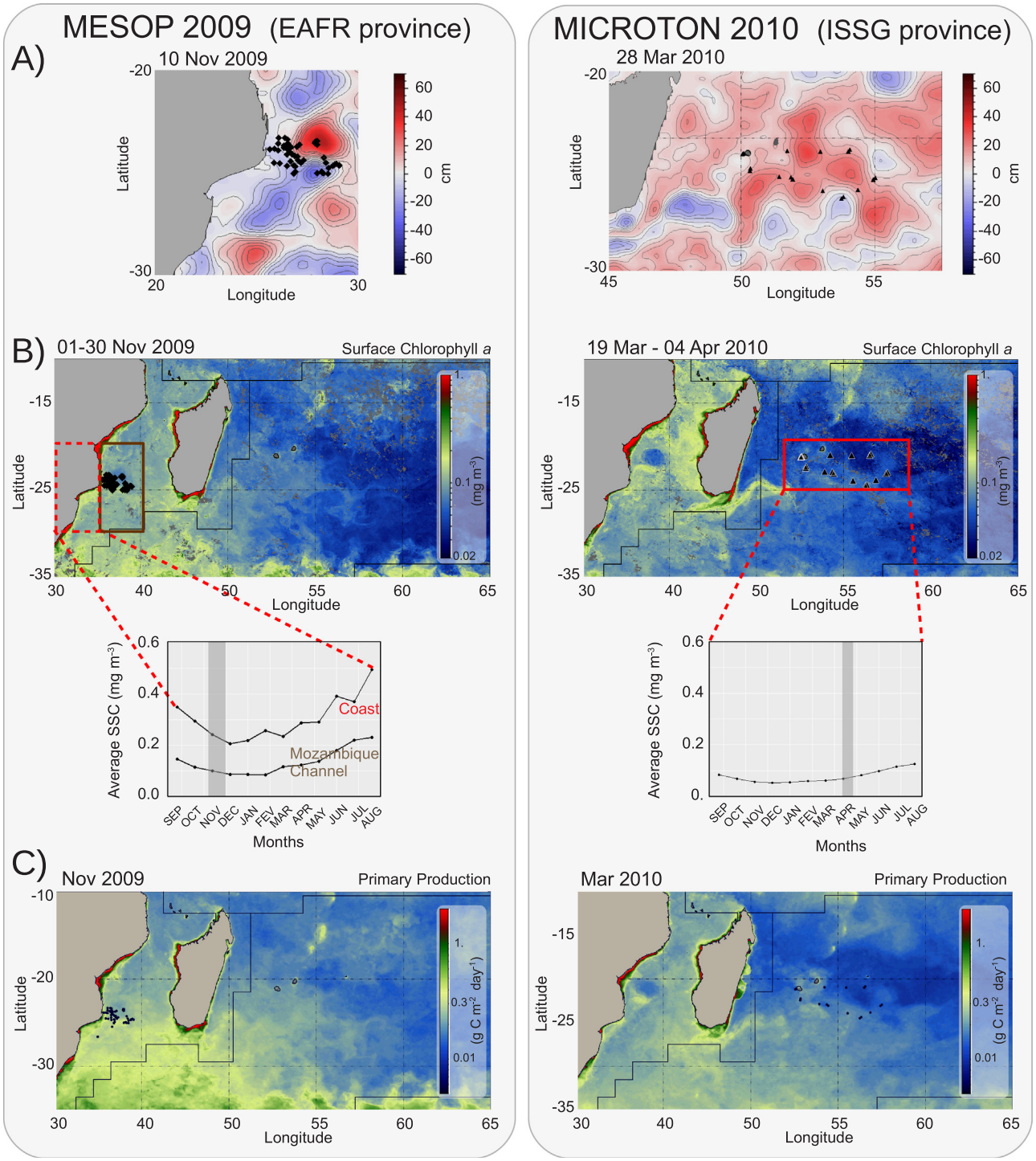

Fig. 2. (A) Sea level anomaly (SLA) maps, dated 28 March 2010 for the MICROTON cruise (left) in the ISSG, and dated 10 November 2009 for the MESOP 2009 cruise (right) in the EAFR, with positive SLA (red) and negative SLA (blue). Color bar indicates the SLA in cm. (B) Averaged satellite image of chlorophyll *a* distribution from 19 March to 4 April 2010 in the ISSG and from 1 to 30 November 2009 in the EAFR with monthly mean chlorophyll *a* values depicted from September 2009 to August 2010 in the region defined in the red squares. The dates of the MICROTON and MESOP cruises are marked by grey bars on the monthly means. Color bar indicates the chlorophyll *a* concentration in mg m^{-3}. (C) Averaged net primary production from 1 to 31 March 2010 for the MICROTON cruise (left) in the ISSG, and from 1 to 30 November 2009 for the MESOP 2009 cruise (right) in the EAFR. Color bar indicates the net primary production in g C m^{-2} day^{-1}. Black symbols represent the position of CTD stations for MICROTON and MESOP 2009.

close to the coast (0.21 mg m^{-3}) and in the Mozambique Channel (0.09 mg m^{-3}), then gradually increased in August 2010, both close to the coast (0.50 mg m^{-3}) and in the Mozambique Channel (0.23 mg m^{-3}). The November MESOP 2009 measurements were taken during a declining phase of oceanic productivity. The net primary production was also greater in the mesotrophic EAFR compared to the oligotrophic ISSG province, both in November 2009 and March 2010 (Fig. 2C).

The mean DCM was deeper across all stations in the ISSG (116.4 ± 11.8 m) than the EAFR (93.8 ± 26.3 m). In both the ISSG and the EAFR, the DCM was shallower in cyclones, intermediate in frontal zones and deeper in anticyclones. The mean thermocline depth was also deeper across all stations in the ISSG (171.3 ± 49.2 m)

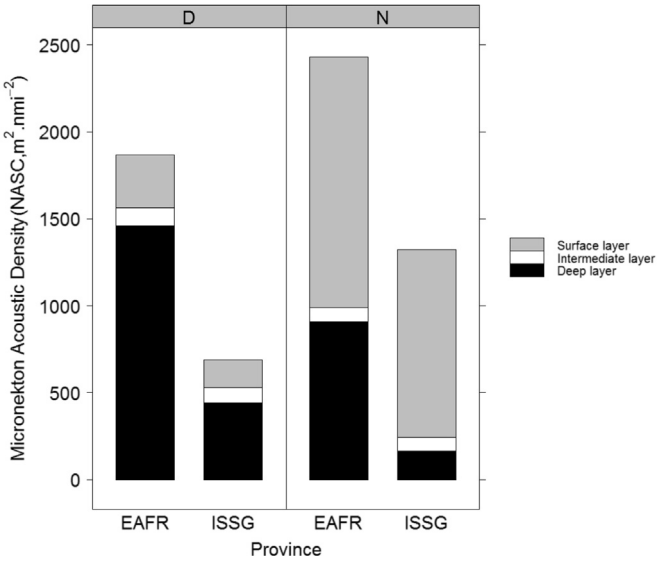

Fig. 3. Mean s_A in the EAFR and the ISSG for day (D) and night (N) sections: grey for the surface layer (10–200 m), white for the intermediate layer (200–400 m), and black for the deep layer (400–740 m).

compared to stations in the EAFR (140.7 ± 59.6 m), with less variation across eddy features in the ISSG.

3.2. DVM of micronekton

Day and night variations in the micronekton vertical distribution were recorded in both the ISSG and the EAFR provinces, illustrating the DVM process. In the ISSG the surface, intermediate and deep layers gathered approximately 23%, 13% and 64% of acoustic densities during the day, and approximately 82%, 6% and 12% respectively at night (Fig. 3). In the EAFR, the surface, intermediate and deep layers gathered approximately 16%, 6% and 78% of acoustic densities respectively during the day, and approximately 60%, 3% and 37% respectively during the night (Fig. 3). Significant differences between day and night in the acoustic densities were recorded in all thirty-seven 10–20-m depth bins ($L_{10–20}$, $L_{20–40}$, $L_{40–60}$….$L_{720–740}$) in the ISSG (Kruskal-Wallis, $H = 31.63$, $n = 643$, $P < 0.05$) and the EAFR (Kruskal Wallis, $H = 82.28$, $n = 349$, $P < 0.05$).

Overall acoustic densities during the day and night between 0 and 740 m were lower in the ISSG than the EAFR (Figs. 3 and 4). During daytime, the mean vertical distribution in the ISSG was uniform, with a total acoustic response of 690 m^2 nmi^{-2} and with 50% and 75% of the micronekton acoustic densities being recorded between the surface and maximum depths of 480 m and 600 m respectively (Fig. 4). At night in the ISSG, 50% and 75% of the acoustic densities were recorded between 100 m and 160 m respectively, with a total acoustic response of 1321 m^2 nmi^{-2}. A difference of 631 m^2 nmi^{-2} was observed between day and night vertical profiles during MICROTON in the ISSG. During MESOP 2009 in the EAFR, a pronounced bi-modal distribution and a total acoustic response of 1866 m^2 nmi^{-2} were recorded during the day (Fig. 4), with the 50% and 75% indicators located at 520 m and 600 m respectively. At night in the EAFR, the 50% and 75% indicators were located at 120 m and 520 m respectively, with a total acoustic response of 2429 m^2 nmi^{-2}. A difference of 563 m^2 nmi^{-2} was observed between the day and night mean vertical profiles during MESOP 2009 in the EAFR. Peaks in micronekton acoustic densities in both provinces were observed in the deep layer at night and in the shallow layer during the day.

3.3. Micronekton assemblage

The overall mean weights of micronekton in the shallow tows at night were lower during MICROTON in the ISSG compared to MESOP 2009 in the EAFR (Fig. 5A). In both provinces, mean wet weight estimates from all deep tows during the day and shallow tows at night, yielded the greatest mean weights of mesopelagic fishes and the gelatinous category (whole individuals and pieces of organisms). In the EAFR, the daytime intermediate depth tows yielded the greatest mean weight of gelatinous individuals and pieces of gelatinous organisms (Fig. 5A).

Micronekton abundance estimates from the 19 day- and night trawls in the ISSG across all depth categories were lower than those in the EAFR, with only 19,900 individuals caught in the ISSG compared to 30,700 individuals caught in the 20 day- and night trawls from the EAFR. Consistent with acoustic recordings, abundance estimates for night-time shallow tows in both provinces were greater than for daytime shallow tows (Fig. 5B). Overall abundance estimates for night-time and daytime shallow tows in the ISSG were also lower than those in the EAFR.

In night-time shallow tows, mesopelagic fishes dominated the total catch in both the ISSG (57% by number) and the EAFR (73% by number) (Figs. 5B and 6). Crustaceans and squids made up the remainder of the catch, with crustacean families being the second most abundant organisms caught in both provinces. Among mesopelagic fishes, Myctophidae were the most represented family in both provinces (Fig. 6). Other dominant mesopelagic fishes included the Phosichthyidae, Gonostomatidae, Sternoptychidae, Stomiidae, Paralepididae, Notosudidae, Bregmacerotidae and fish larvae. The mesopelagic fish families Engraulidae, Nomeidae, Scombrolabracidae, Bramidae and Carangidae were caught in the EAFR only.

In night-time deep tows, crustaceans dominated the total catch both in the ISSG (61% by number) and the EAFR (63% by number) (Fig. 6). In the ISSG, a variety of crustaceans: was caught, including Caridea, Euphausiacea, *Oplophorus*, Sergestidae, *Gennadas* spp., Oplophoridae and *Funchalia* (Fig. 6). In the EAFR, several crustacean taxa were abundantly caught in night-time deep tows: *Platyscelus*, *Thysanopoda*, *Brachyscelus* and *Oxycephalus*. Gelatinous organisms are under-represented in net counts because most species break apart in the nets.

3.4. Environmental drivers of micronekton variability

The CCA analysis showed that 29.7% of the variability in the micronekton species distribution is explained by sea surface chlorophyll (SSC), minimum oxygen concentration (MinOxy), minimum oxygen depth (MinOxy.Depth), deep chlorophyll maximum depth (DCM.depth), sea surface temperature (SST), sea level anomaly (SLA) and thermocline depth (Thermocline.Depth) (Fig. 7). The first canonical axis, CCA1, accounted for 45.6% of the species-environment relationship. The strongest correlations were between CCA1 and SSC (-0.76), minimum oxygen concentration (0.90) and SST (0.85). Adding the second axis, CCA2, accounted for 68% of the cumulative variation; CCA2 showed a strong negative correlation with the thermocline depth (-0.57) (Supplementary information, Table 2). The pattern for most of the oligotrophic MICROTON (ISSG) stations, with deep, reduced fluorescence values, deep thermoclines, warm SSTs and elevated minimum oxygen concentrations, is opposite to that for the more productive MESOP 2009 (EAFR) stations, which have high SSCs. Most micronekton species sampled (red crosses, Fig. 7) are associated with high SSCs, but several species are also associated with elevated SLAs, and deep DCMs and thermoclines.

3.5. $\delta^{15}N$ and $\delta^{13}C$ signatures

During MICROTON in the ISSG, clear segregations were observed among POM, zooplankton, gelatinous organisms, micronekton

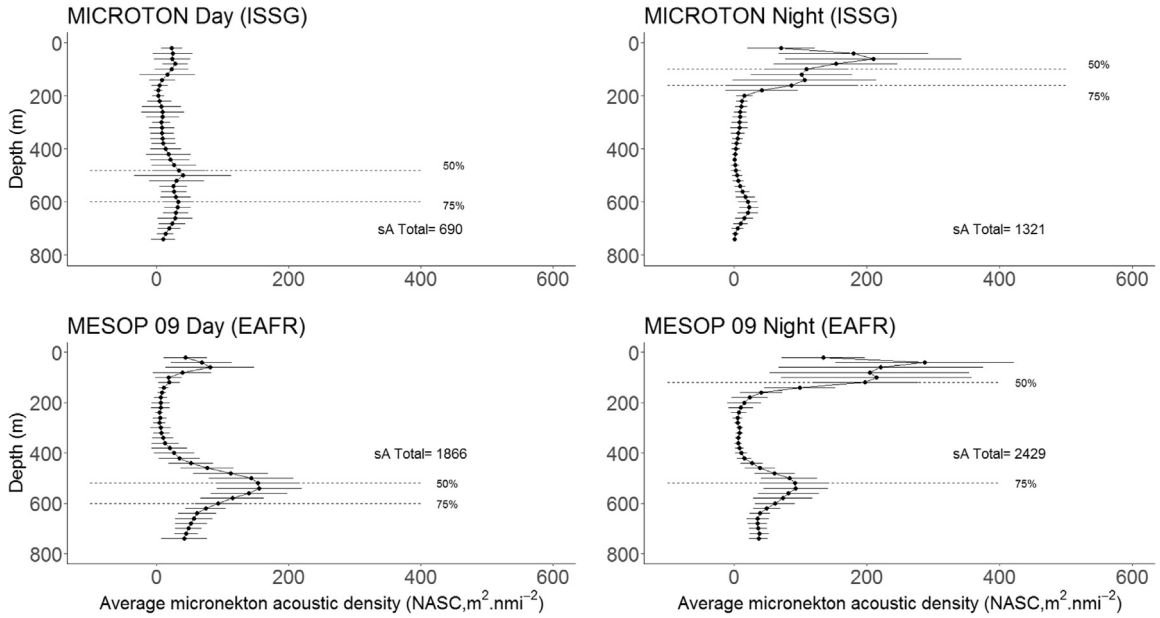

Fig. 4. Mean ± (S.D.) vertical profiles during day and night in the ISSG and the EAFR. The indicators 50% and 75% show the maximum depths reached by 50% and 75% of the acoustic densities cumulated from the sea surface. The total acoustic responses are given in m^2 nmi^{-2}.

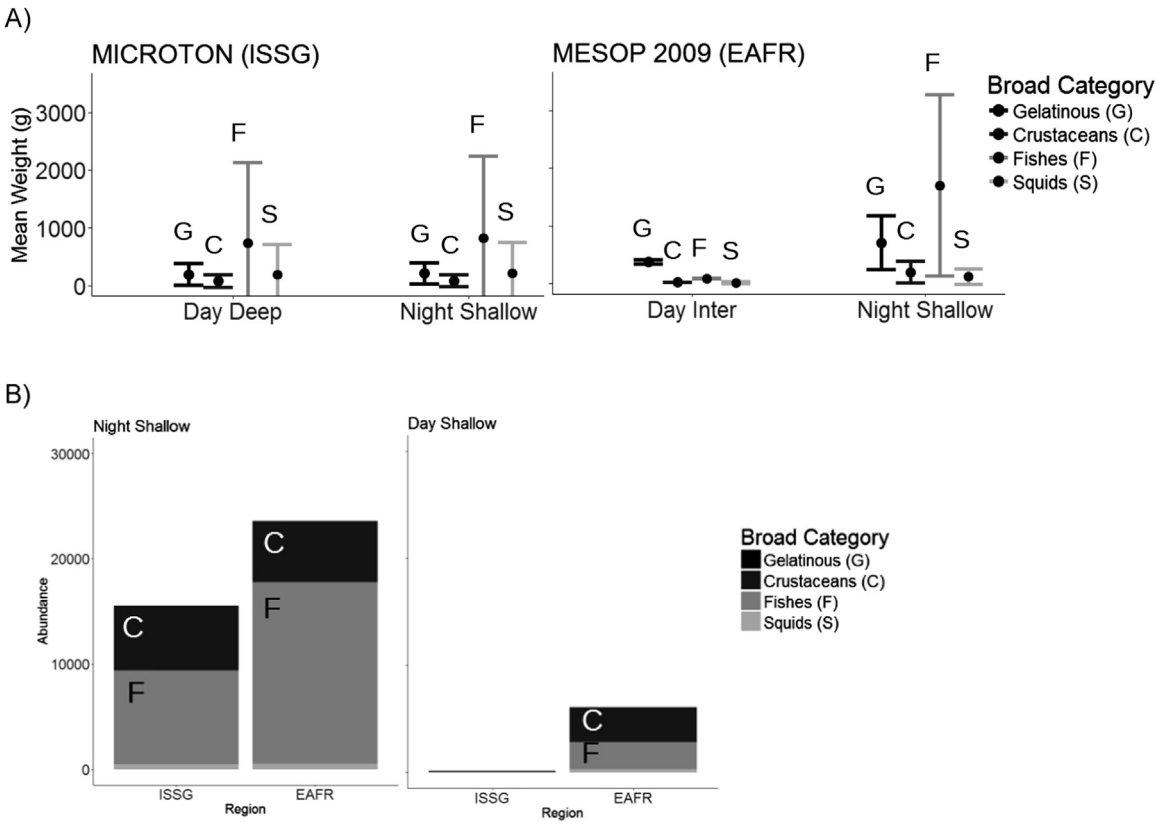

Fig. 5. (A) Mean weight estimates (g) of gelatinous organisms (G), crustaceans (C), fishes (F) and squids (S) in shallow night-time (0–200 m) and deep daytime trawls (below 400 m) in the ISSG and the EAFR and daytime intermediate-depth trawls (200–400 m) in the EAFR. (B) Overall abundance of micronekton in shallow night-time and shallow day-time trawls in the ISSG and the EAFR.

(crustaceans, fishes and squids) and swordfish in both $\delta^{15}N$ (Kruskal-Wallis, H = 444.2, df = 8, P < 0.05) and $\delta^{13}C$ values (Kruskal-Wallis, H = 0.482.0, df = 8, P < 0.05). In the EAFR, POM, gelatinous organisms, micronekton (crustaceans, fishes and squids) and swordfish were also segregated according to their $\delta^{15}N$ (Kruskal-Wallis, H = 287.0, df = 6, P < 0.05) and $\delta^{13}C$ signatures (Kruskal-Wallis, H = 326.4, df = 6, P < 0.05).

During MESOP 2009 in the EAFR, surface POM (POM-Surf) had higher mean $\delta^{15}N$ values (8.0 ± 1.1‰) than POM collected at the fluorescence maximum (POM-Fmax: 5.0 ± 1.3‰). Surface POM in the EAFR also had higher $\delta^{15}N$ values than POM-Surf (6.3 ± 0.8‰) and POM-Fmax (5.6 ± 0.9‰) from the ISSG (Fig. 8). In the EAFR, POM-

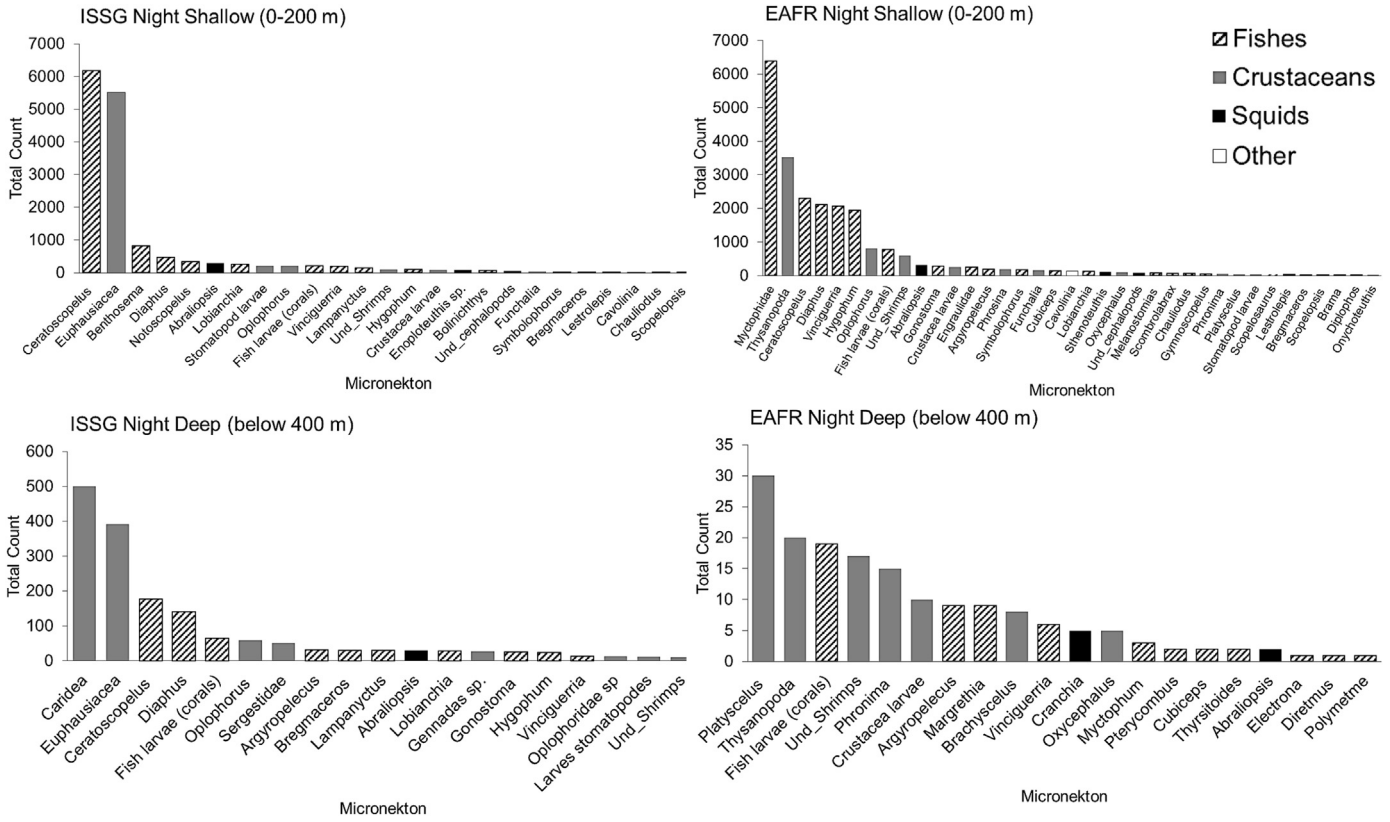

Fig. 6. Frequency distribution of the most abundant species of micronekton in shallow night-time (0–200 m) and deep night-time (below 400 m) trawls in the ISSG and the EAFR.

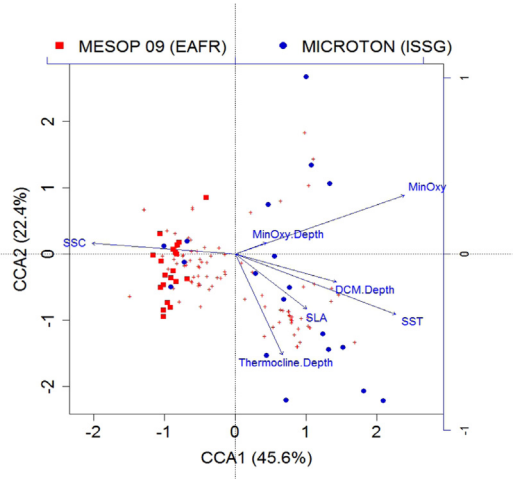

Fig. 7. Canonical correspondence analysis (CCA) ordination diagram of the micronekton species (red crosses). The trawl stations are shown as red squares for MESOP 2009 and blue dots for MICROTON. The blue arrows indicate significant explanatory variables, from a set of environmental descriptors (sea surface chlorophyll, minimum oxygen concentration, sea surface temperature, sea level anomaly, thermocline depth, deep chlorophyll maximum depth and minimum oxygen depth). The arrowheads indicate the direction of increasing gradient.

Surf and POM-Fmax were spread over a wider range of $\delta^{13}C$ values (-26.3 to -22.0‰ and -25.3 to -21.0‰ respectively), than were found in the ISSG province (POM-Surf: -24.5 to -23.6‰; POM-Fmax: -25.4 to -23.3‰). In the EAFR, the chlorophyll *a* concentrations were the foremost explanatory variables of the variability in POM $\delta^{13}C$ ($F_{51,\ 3}$ = 2.812, $P < 0.05$) and POM $\delta^{15}N$ values ($F_{51,\ 3}$ = 41.69, $P < 0.05$). In the ISSG, variability in POM $\delta^{13}C$ and $\delta^{15}N$ values could not be explained by any of the selected explanatory variables ($\delta^{13}C$: $F_{24,\ 3}$ = 7.279, $P > 0.05$; $\delta^{15}N$: $F_{24,\ 3}$ = 2.099, $P > 0.05$).

In the ISSG and the EAFR, gelatinous organisms had the largest isotopic niche widths (ISSG: SEA_c = 6.40; EAFR: SEA_c = 9.05) compared to all other components of the food web (Fig. 8). The $\delta^{15}N$ values of crustaceans, fishes and squids ranged from 3.0‰ (Leptocephali larvae) to 13.5‰ (the squid *H. hoylei*) in the ISSG, and from 4.7‰ (Leptocephali larvae) to 16.6‰ (the fish *Decapterus* spp.) in the EAFR (Supplementary information, Table 1). Pairwise comparisons indicated that crustaceans, fishes and squids in the ISSG did not differ significantly in their $\delta^{15}N$ values ($P > 0.05$), but isotopic niche widths were more similar for mesopelagic fishes and squids (SEA_c = 2.94 and 2.90 respectively) than crustaceans (SEA_c = 1.56). In the EAFR, crustaceans differed from fishes and squids in their $\delta^{15}N$ signature ($P < 0.05$) and isotopic niche width value (SEA_c = 1.76), whereas fishes and squids had similar $\delta^{15}N$ values ($P > 0.05$) and isotopic niche widths (fishes: SEA_c = 2.28; squids: SEA_c = 1.90).

3.5.1. *Trophic level estimates of micronekton*

During MICROTON in the ISSG province, an average ^{15}N enrichment of 3.4‰ (calculated from the difference in $\delta^{15}N$ values) was observed between zooplankton and micronekton (crustaceans, fishes and squids). The average calculated TLs of zooplankton and micronekton were 2.0 and 3.1 respectively, suggesting that these two groups were found at successive trophic levels. Estimated TLs of micronekton ranged from 1.4 (Leptocephali larvae) to 4.6 (*H. hoylei*), with estimated TL values exhibiting the same pattern as $\delta^{15}N$ signatures because the two variables are linearly related (Eq. (2)). During MESOP 2009 in the EAFR, micronekton (crustaceans, fishes and squids) had an average estimated TL value of 3.3, ranging from 1.8 (Leptocephali larvae) to 5.5 (*Decapterus* spp.) (Supplementary information, Table 1). The average calculated TL values of crustaceans, fishes and squids were 2.9, 3.1 and

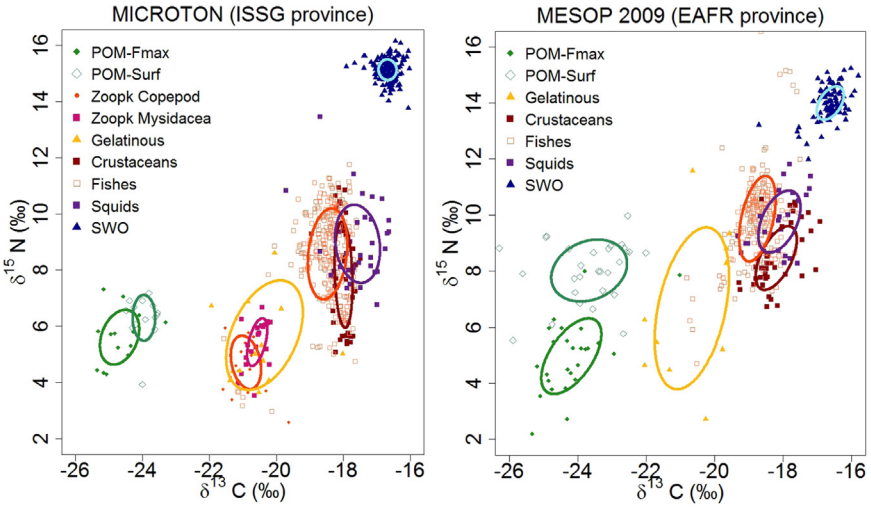

Fig. 8. Bivariate plots of $\delta^{15}N$ and $\delta^{13}C$ values (‰) for particulate organic matter at the deep chlorophyll maximum (Fmax) and at the surface (Surf), copepods, mysids, gelatinous organisms, crustaceans, mesopelagic fishes, squids and swordfish in the ISSG and the EAFR. Standard ellipse areas (colored solid lines), calculated using SIBER, provide estimates of the size of the isotopic niche for each of these categories.

3.2 respectively in the ISSG and 3.0, 3.5 and 3.4 respectively in the EAFR.

3.5.2. Swordfish trophic position

During MICROTON in the ISSG, a difference of 6.6‰ in $\delta^{15}N$ values was calculated between micronekton (crustaceans, fishes and squids: average $\delta^{15}N$ value of 8.5‰) and swordfish (average $\delta^{15}N$ value of 15.1‰), which is approximately twice the reference average enrichment value of 3.2‰ between consecutive trophic levels. In the ISSG, swordfish specimens had higher $\delta^{15}N$ and a higher estimated TL (5.2) than the other components of the food web; the range in $\delta^{15}N$ values of swordfish was 13.8‰ to 16.2‰ in the ISSG. During MESOP 2009 in the EAFR, a difference of 4.3‰ was calculated between micronekton (average $\delta^{15}N$ value of 9.7‰) and swordfish (average $\delta^{15}N$ value of 14.0‰), with some overlap in $\delta^{15}N$ values between several squids and mesopelagic fishes (Fig. 8). In the EAFR, swordfish specimens had a range in $\delta^{15}N$ values of 12.0‰ to 15.2‰ and an average TL of 4.7, which is lower than the TL of some of the mesopelagic fishes sampled (Supplementary information, Table 1).

The $\delta^{15}N$ values of swordfish differed significantly as a function of size and region (linear model, $F_{265} = 253.2$, $P < 0.05$). In the ISSG province, swordfish specimens less than 1000 mm (n = 1), between 1000 and 2000 mm (n = 148) and greater than 2000 mm (n = 23), had average $\delta^{15}N$ values of 15.6‰, 15.1 ± 0.4‰ and 15.3 ± 0.3‰ respectively and TL estimates of 5.3, 5.2 and 5.2 respectively. In the EAFR, swordfish specimens less than 1000 mm (n = 4), between 1000–2000 mm (n = 85) and greater than 2000 mm (n = 7), had average $\delta^{15}N$ signatures of 12.7 ± 0.5‰, 14.0 ± 0.5‰ and 14.3 ± 0.5‰ respectively and TL estimates of 4.3, 4.8 and 4.8 respectively.

3.5.3. Effect of feeding regime on isotopic signatures of micronekton

Within the ISSG and the EAFR provinces, micronekton organisms with different feeding regimes had significantly different $\delta^{15}N$ (ANOVA, ISSG: $F_{3,\ 341} = 38.0$, $P < 0.05$; EAFR: $F_{3,\ 267} = 38.8$, $P < 0.05$) and $\delta^{13}C$ (ANOVA, ISSG: $F_{3,\ 341} = 74.5$, $P < 0.05$; EAFR: $F_{3,\ 267} = 80.5$, $P < 0.05$) values. Carnivorous organisms (mostly mesopelagic fishes and squids) and omnivorous organisms (mostly crustaceans) had lower average $\delta^{15}N$ values in the ISSG (8.8 ± 1.5‰ and 7.8 ± 1.7‰ respectively) than the EAFR (9.9 ± 1.4‰ and 8.6 ± 1.1‰ respectively). Detritivores (Leptocephali larvae) and filter feeders (*Salpa maxima* and *Pyrosomatida*) also had lower average $\delta^{15}N$ values in the ISSG (3.3 ± 0.3‰ and 5.7 ± 1.9‰) compared to the EAFR (6.3 ± 1.2‰ and 5.8 ± 2.8‰ respectively).

3.5.4. Body size effect on $\delta^{15}N$ signatures of micronekton

There were no clear relationships between $\delta^{15}N$ values of micronekton (crustaceans, fishes and squids) and body size from samples collected both in the ISSG (linear model, $F_{341} = 1.529$, $P > 0.05$) and in the EAFR (linear model, $F_{264} = 0.2226$, $P > 0.05$). The $\delta^{15}N$ signatures of the selected fishes *C. warmingii*, *V. nimbaria*, *D. richardsoni* and *H. hygomii*, the crustacean *Funchalia* spp. and the squid *S. oualaniensis*, did not differ as a function of size ($F_{179} = 3.142$, $P > 0.05$) but differed as a function of region ($F_{181} = 49.3$, $P < 0.05$). For the same body lengths, the selected specimens had higher $\delta^{15}N$ values in the EAFR compared to the ISSG (Fig. 9).

4. Discussion

This study illustrated differences in the structure and the dynamics of micronekton communities and their consequences for food web functioning in an oligotrophic biogeochemical province and a more productive one. The results are in accordance with our hypotheses and highlight the importance of river inputs and mesoscale eddies in the biological production of pelagic ecosystems.

4.1. Sampling bias and constraints

Although the patterns are clear, several potential biases are recognised in this study, notably linked to spatio-temporal variability in the distribution of each broad micronekton category and temporal variability in the data acquisition between the cruises. Acoustic recordings, mid-water trawls and stable isotope analyses all present certain limitations. Acoustic recordings are sensitive to weather conditions, swells and wind stress, thus limiting the echo-integration of the 38 kHz transducer acoustic data to 740 m, making it impossible to observe the secondary deep scattering layer, which is usually located at approximately 825 m (Proud et al., 2017). Some groups were poorly represented: squids and crustaceans are capable of net avoidance and gelatinous organisms can be damaged in net tows, biasing the determination of micronekton community compositions in both provinces. Isotopic TL calculations can also present several caveats because isotopic baselines can vary seasonally and spatially (Ménard et al., 2014) and the rate at which organisms incorporate the isotopic signal of their diets into their tissues can vary among organisms and among the tissues within a single individual (Martínez Del Rio et al., 2009). The application of a fixed average enrichment factor of 3.2‰ can lead to errors in TL estimations since the ^{15}N enrichment per trophic level has been shown to become smaller in the upper parts of a food web (Hussey et al., 2014). Nevertheless, for consistency and comparability with other studies, a fixed enrichment factor, averaged across numerous

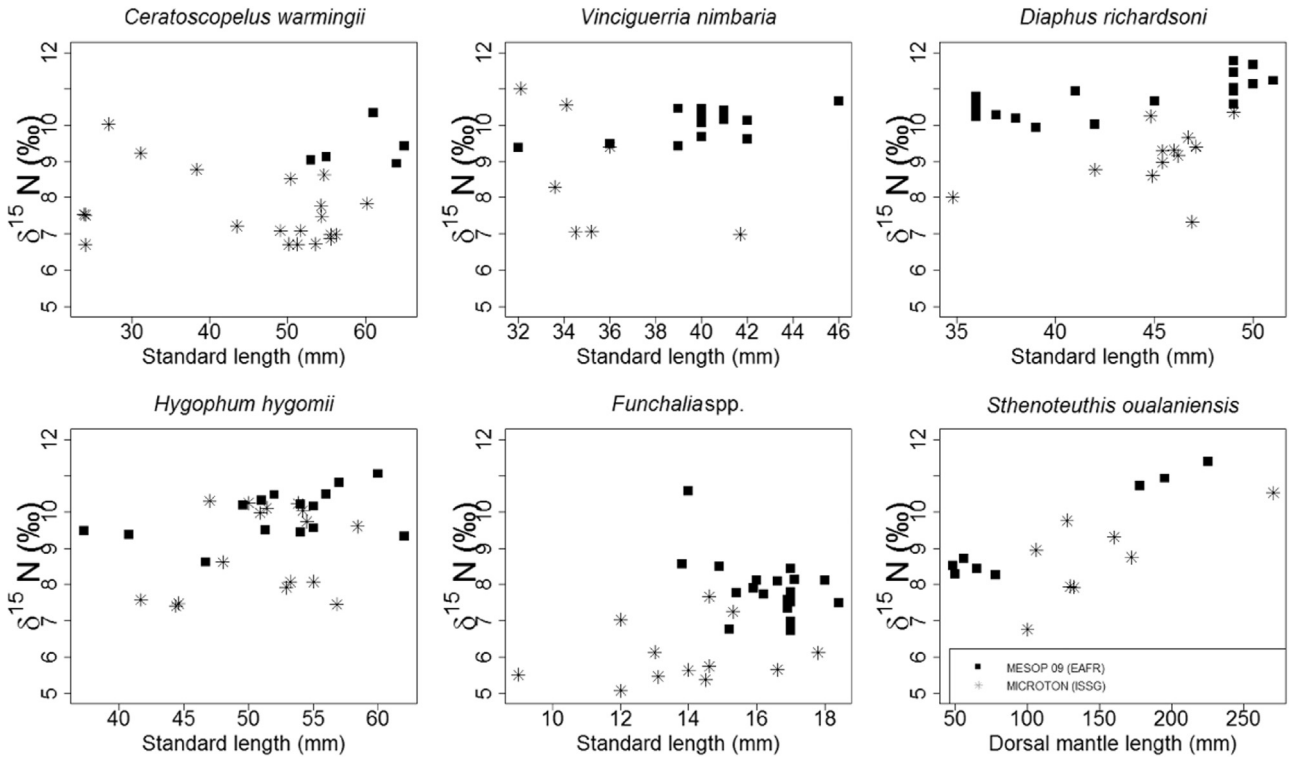

Fig. 9. δ^{15}N values (‰) from the fishes, *Ceratoscopelus warmingii*, *Vinciguerria nimbaria*, *Diaphus richardsoni*, *Hygophum hygomii*, the crustacean *Funchalia* spp. and the squid *Sthenoteuthis oualaniensis* plotted against body lengths in mm (standard lengths for fishes and the crustacean and dorsal mantle lengths for the squid) in the EAFR (squares) and the ISSG (star symbols).

studies and species, is used (Minagawa and Wada, 1984; Post, 2002).

4.2. Oceanography

This study highlighted contrasting environmental patterns in the ISSG and the EAFR provinces. In the ISSG, the ocean dynamics at a small scale are mainly dominated by anticyclonic mesoscale eddies of low amplitude (~ 10 cm), which create physical downwelling that leads to a deep DCM and thermocline, with occasional shoaling of the latter in the presence of a few cyclonic eddies. In the ISSG, the prevailing environmental feature at a larger scale is a subtropical (anticyclonic) gyre that pushes nutrients and chlorophyll deeper in the water column (Stramma and Lutjeharms, 1997; Jena et al., 2013; Pous et al., 2014). In contrast, the EAFR province is a more dynamic system, with the presence of intense cyclonic and anticyclonic eddies propagating southwards, leading to varied DCM- and thermocline depths. In situ chlorophyll *a* data and remote sensing data have shown that year-round productivity is enhanced in the EAFR compared to the ISSG, although the chlorophyll *a* seasonal cycles are similar in both provinces. Remote sensing data have also shown enhanced productivity at the Mozambique Coast, which is most likely caused by riverine input. This production can be entrained by mesoscale eddies in the Mozambique Channel (filaments being driven off the coast observed in Fig. 2B). Surface currents and EKEs were very strong during the MESOP 2009 cruise in the EAFR. The enhanced EKE associated with mesoscale eddies previously has been shown to occasionally drive the entrainment of chlorophyll-enriched coastal waters into the Mozambique Channel (Tew-Kai and Marsac, 2009; Zubkov and Quartly, 2003; Kolasinski et al., 2012, see Fig. 2B). Cyclonic eddies also create an upward displacement of cold, nutrient-rich waters (McGillicuddy et al., 1998; Oschlies and Garcon, 1998; Bakun, 2006), further contributing to the overall productivity in the EAFR (Kolasinski et al., 2012).

The CCA analyses showed strong association of micronekton species with high SSCs. The enhanced eddy activity and its associated high productivity in the EAFR might favour a greater abundance of micronekton as compared to that in the ISSG (total s_A recorded, wet weight estimates and total net abundance estimates were higher in the EAFR compared to the ISSG). Eddies are known to provide mechanisms whereby the physical energy of the ocean system is converted into trophic energy, supporting biological processes (Bakun, 2006; Barlow et al., 2014; Huggett, 2014).

4.3. Influence of environmental parameters on micronekton DVM

Acoustic responses were distributed in the upper 200 m of the water column at night, and below 400 m (in the EAFR) or 800 m (in the ISSG) during the day. The majority of acoustic responses detected in both provinces can be attributed to migrant micronekton (Béhagle et al., 2014). The total acoustic responses were greater at night compared to the day in both provinces, suggesting that some micronekton communities migrate from layers deeper than 740 m, i.e. beyond the range set for the 38 kHz transducer (as in Béhagle et al., 2014; Proud et al., 2017). Other possibilities might include horizontal advection of free swimming micronekton organisms (Benoid-Bird and Au, 2006). Previous studies in other oceanic regions have shown that vertical migration can further be influenced by light (Andersen et al., 1998; Olivar et al., 2012), productivity and oxygen minima (Ekau et al., 2010; Olivar et al., 2017), temperature (Youngbluth, 1975), food (Bernal et al., 2015), and clear oligotrophic waters where organisms will dive deeper at dawn to avoid visual predation (Andersen et al., 1998).

The peak observed in the night-time mean acoustic profiles at 600 m in the ISSG and 580 m in the EAFR could correspond to organisms still migrating from deeper layers at the time that the data were recorded or to non-migrant micronekton organisms that do not ascend at dusk. Gelatinous organisms (having a non-negligible response to the 38 kHz frequency), some fishes from the Myctophidae family (*Lampanyctus* spp. and *S. nannochir*) (Watanabe et al., 1999), the majority of stomiiform species (*Argyropelecus* spp., *C. sloani* and *Vinciguerria* spp.) (Benoid-Bird

and Au, 2006; Olivar et al., 2012, 2017), and some carids and sergestids (Kikuchi and Omori, 1985) have been reported to be non-migrants or partially- migrating species. Crustaceans of the order Euphausiacea and *Gennadas* spp. have also been shown to exhibit a bi-modal distribution, being located between 100–200 m and 450–550 m at night (Andersen et al., 1998). The 11–30 mm gonostomatid *Cyclothone* spp., poorly sampled in our study because of the large mesh-size net used, is known to be abundant in the 400–600 m depth range during both the day and night, and represents an important acoustic backscatter at this depth (Andersen et al., 1998; Olivar et al., 2012, 2017). A permanent deep thermocline in the ISSG could also limit the upward migration of some species, such as the crustacean *Thysanopoda* spp., that are sensitive to the thermocline depth (Youngbluth, 1975).

4.4. Trophic structuring of the ISSG and the EAFR

POM $\delta^{13}C$ and $\delta^{15}N$ values in the EAFR showed a wider range than in the ISSG (Fig. 8). This might suggest both terrestrial and marine inputs of productivity in the EAFR. In contrast to previous studies where $\delta^{15}N$ of POM increased with depth (Mintenbeck et al., 2007; Fanelli et al., 2013), surface POM had higher $\delta^{15}N$ values than POM-Fmax in the EAFR. The stable isotope composition of POM, a proxy for primary producers (Seyboth et al., 2017), is also correlated with chlorophyll *a* in the more productive EAFR province but not in the ISSG. The combined action of riverine input and the dynamics of mesoscale eddies that drive nutrient-rich coastal waters in the Mozambique Channel and cause significant upwelling, bringing nitrate (high in $\delta^{15}N$) to the surface where it is utilized by phytoplankton, can enhance POM $\delta^{15}N$ values in the EAFR compared to the ISSG. Previous studies have shown that seaweed detritus and coastal diatoms have a significant contribution to the inshore POM pool in the Mozambique Channel, leading to enriched values (Kolasinski et al., 2012). Eutrophic waters have been shown to be nitrate-dominated and to be enriched in ^{15}N (Checkley and Entzeroth, 1985), resulting in zooplankton being enriched in ^{15}N (Mullin et al., 1984). In oligotrophic waters such as the ISSG, primary production may be largely dependent on recycled and depleted ^{15}N (Polunin et al., 2001) or on cyanobacteria fixing atmospheric nitrogen (Karl et al., 1997), yielding lower POM $\delta^{15}N$ values.

The high variability in isotopic signatures found at the base of the food web is likely reflected at higher trophic levels (Stowasser et al., 2012), with an enrichment of consumer tissues in the EAFR. In both provinces, detritivores (Leptocephali larvae) and filter feeders were less enriched in $\delta^{13}C$ and $\delta^{15}N$ compared to omnivores (mostly crustaceans) and carnivores (mostly mesopelagic fishes and squids and the gelatinous Siphonophora). Filter feeding gelatinous organisms such as *Pyrosomatida* and *S. maxima* caught in the EAFR in daytime at intermediate depths (200–400 m) and night-time during shallow tows (0–200 m) showed large niche widths and great variability in their $\delta^{15}N$ values, suggesting ingestion of a variety of suspended particles. Carnivorous organisms in the EAFR probably became enriched in ^{15}N because of an enriched food base and to the ^{15}N enrichment in tissues at each intermediate trophic step. The large span of crustaceans' niche widths in the ISSG province further suggests feeding on a variety of prey items. An omnivorous feeding mode would be beneficial to organisms dwelling in the oligotrophic ISSG province because they can prey on zooplankton, euphausiids and copepods and also on various types of phytoplankton. Some deep dwelling organisms such as *Cyclothone* spp., are known to feed primarily on a suspended particle-based food web (Gloeckler et al., 2017). Vertically migrant micronekton, feeding on ^{15}N-enriched organic material at the surface in the EAFR and defecating at depth, can contribute to ^{15}N enrichment of the tissues of these deep dwelling consumers. Further studies are required to test this hypothesis.

Body length has been shown to influence $\delta^{15}N$ values in previous studies because, as they grow in size, some organisms can feed on larger prey with greater $\delta^{15}N$ signatures (Parry, 2008). In this study, no significant body length effect on micronekton $\delta^{15}N$ values was observed in the ISSG and the EAFR, suggesting high overlap in the diet between species of different sizes in both provinces. However, organisms of the same size with the same feeding mode exhibited higher $\delta^{15}N$ values in the more productive EAFR compared to the oligotrophic ISSG province, and hence might be more enriched in ^{15}N (Fig. 9).

The total range of $\delta^{15}N$ values revealed a food web characterised by four trophic levels in the ISSG (i.e. zooplankton and gelatinous organisms = TL2, micronekton = TL3, swordfish = TL5) and three trophic levels in the EAFR (i.e. gelatinous organisms = TL2, micronekton = TL3 and swordfish = TL4). TL 4 specimens have been weakly sampled in the ISSG (apart from two squids *Histioteuthis* spp.). It is likely that the apparent "gap" in niche space (i.e. above micronekton and below swordfish, Fig. 8) in the ISSG would have been partially filled had the full suite of component species and maturity stages been analysed in this food web.

The apparent "gap" in niche space in the ISSG vs. the overlap between micronekton and swordfish in the EAFR, can be further attributed to the difference in the food availability in the two provinces. *Xiphias gladius* has been reported to feed mainly on other fish species, such as *Cubiceps pauciradiatus* (Potier et al., 2008), and squids, such as *Sthenoteuthis oualaniensis* and *Ommastrephes bartramii* (Stillwell and Kohler, 1985; Ménard et al., 2013; Potier et al., 2014). In low-productive ecosystems such as the ISSG, swordfish can show foraging specialization on large nekton, such as *Ommastrephes* (Ménard et al., 2013), which provide more energy compared to smaller organisms present at lower densities. Swordfish may not be able to broaden their food spectrum in the ISSG because micronekton prey density is reduced and the costs associated with finding prey items are higher than the energy intake when consuming those organisms. The tissues of swordfish samples would thus be more enriched in ^{15}N in the ISSG as a result of foraging on TL 4 squid specimens. The higher abundance of resources in the EAFR region may lead to swordfish enlarging their food spectrum by feeding on lower trophic level prey items that are more readily available (unpublished data). Further studies on swordfish migration and their diets are required to test these hypotheses.

To our knowledge, this study is the first to combine acoustics, ground-truth data using trawls and stable isotope analyses to investigate the spatial distribution and community composition of micronekton, and their role in the trophic web of the productive, coastal EAFR province on the one hand, and of the oligotrophic, oceanic ISSG province on the other hand. Micronekton distribution and abundance in the South West Indian Ocean have been shown to be strongly influenced by SSC. The enrichment mechanisms in the EAFR, contributing to available primary productivity, led to an enrichment of basal organisms in $\delta^{13}C$ and $\delta^{15}N$ values. This translated into enrichment in the selected consumer tissues, with organisms of the same size and with the same feeding mode exhibiting higher $\delta^{15}N$ values in the EAFR compared to the ISSG. However, enrichment processes of consumer tissues stopped at the level of top predators. Enrichment of swordfish tissues in $\delta^{15}N$ values was shown to be strongly influenced by the size of the predator and its hypothesized contrasting dietary habits in the two provinces. Several research directions should be pursued to improve current knowledge about the role of micronekton in high sea ecosystem functioning, including the effects of seasonality and lunar patterns on micronekton biomass, distribution and diversity; the differences of scaled versus additive $\delta^{15}N$ frameworks in trophic level estimations; and detailed studies of swordfish stomach contents.

Acknowledgements

The authors would like to acknowledge all the work carried out by the scientific/non-scientific staff on board the R/V *ANTEA*, the staff members who analysed the samples collected at sea and who played a key role in the stable isotope analyses and acoustic processing of the data collected at sea. This work was mainly supported by the WIOMSA (MARG-II Grant 2013), IRD through the International Centre for

Education, Marine and Atmospheric Sciences Over Africa (ICEMASA) and the Marine Research Institute (Ma-Re) at the University of Cape Town. The authors wish to thank IRD colleague Michel Potier for support in this work and Pierre Richard from LIENSS for carrying out the stable isotope analyses.

Appendix A. Supplementary material

Supplementary data associated with this article can be found in the online version at doi:10.1016/j.dsr.2018.07.002.

References

Andersen, V., François, F., Sardou, J., Picheral, M., Scotto, M., Nival, P., 1998. Vertical distributions of macroplankton and micronekton in the Ligurian and Tyrrhenian Seas (northwestern Mediterranean). Oceanol. Acta 21, 5.

Arkhipkin, A.I., Laptikhovsky, V.V., Bespyatykh, A.V., Murzov, S.A., 1998. Growth, reproduction and feeding of the tropical squid *Ornithoteuthis antillarum* (Cephalopoda, Ommastrephidae) from the central-east Atlantic. Sci. Mar. 62 (3), 273–288. https://doi.org/10.3989/scimar.1998.62n3273.

Ariza, A., Garijo, J.C., Landeira, J.M., Bordes, F., Hernandez-Leon, S., 2015. Migrant biomass and respiratory carbon flux by zooplankton and micronekton in the subtropical northeast Atlantic Ocean (Canary Islands). Prog. Oceanogr. 134, 330–342. https://doi.org/10.1016/j.pocean.2015.03.003.

Bakun, A., 2006. Fronts and eddies as key structures in the habitat of marine fish larvae: opportunity, adaptive response and competitive advantage. Sci. Mar. 70S2, 105–122. https://doi.org/10.3989/scimar.2006.70s2105.

Barlow, R., Lamont, T., Morris, T., Sessions, H., van den Berg, M., 2014. Adaptation of phytoplankton communities to mesoscale eddies in the Mozambique channel. Deep-Sea Res. Part II: Top. Stud. Oceanogr. 100, 106–118. https://doi.org/10.1016/j.dsr2.2013.10.020.

Beaugrand, G., Ibañez, F., Lindley, J.A., Reid, P.C., 2002. Diversity of calanoid copepods in the North Atlantic and adjacent seas: species associations and biogeography. Mar. Ecol. Progr. Ser. 232, 179–195. ⟨http://www.jstor.org/stable/24865161⟩.

Béhagle, N., Du Buisson, L., Josse, E., Lebourges-Dhaussy, A., Roudaut, G., Ménard, F., 2014. Mesoscale features and micronekton in the Mozambique Channel: an acoustic approach. Deep-Sea Res. Part II: Top. Stud. Oceanogr. 100, 164–173. https://doi.org/10.1016/j.dsr2.2013.10.024.

Behrenfeld, M.J., Westberry, T.K., Boss, E.S., O'Malley, R.T., Siegel, D.A., Wiggert, J.D., Franz, B.A., McClain, C.R., Feldman, G.C., Doney, S.C., Moore, J.K., Dall'Olmo, G., Milligan, A.J., Lima, I., Mahowald, N., 2009. Satellite-derived fluorescence reveals global physiology of ocean phytoplankton. Biogeosciences 6, 779–794. https://doi.org/10.5194/bg-6-779-2009.

Benoid-Bird, K., Au, W.W.L., 2006. Extreme diel horizontal migrations by a tropical nearshore resident micronekton community. Mar. Ecol. Progr. Ser. 319, 1–14. https://doi.org/10.3354/meps319001.

Bernal, A., Olivar, M.P., Maynou, F., Fernández de Puelles, M.L., 2015. Diet and feeding strategies of mesopelagic fishes in the western Mediterranean. Progr. Oceanogr. 135, 1–17. https://doi.org/10.1016/j.pocean.2015.03.005.

Bertrand, A., Bard, F.X., Josse, E., 2002. Tuna food habits related to the micronekton distribution in French Polynesia. Mar. Biol. 140, 1023–1037.

Bianchi, D., Stock, C., Galbraith, E.D., Sarmiento, J.L., 2013. Diel vertical migration: ecological controls and impacts on the biological pump in a one-dimensional ocean model. Glob. Biogeochem. Cycles 27 (2), 478–491. https://doi.org/10.1002/gbc.20031.

Bodin, N., Budzinski, H., Le Ménach, K., Tapie, N., 2009. ASE extraction method for simultaneous carbon and nitrogen stable isotope analysis in soft tissues of aquatic organisms. Anal. Chim. Acta 643 (1–2), 54–60.

Brodeur, R., Yamamura, O., 2005. PICES Scientific Report No. 30 Micronekton of the North Pacific. 30. PICES Scientific Report, Sidney, B.C., Canada, pp. 1–115.

Catul, V., Gauns, M., Karuppasamy, P.K., 2011. A review on mesopelagic fishes belonging to family Myctophidae. Rev. Fish Biol. Fish. 21 (3), 339–354. https://doi.org/10.1007/s11160-010-9176-4.

Checkley Jr., D.M., Entzeroth, L.C., 1985. Elemental and isotopic fractionation of carbon and nitrogen by marine, planktonic copepods and implications to the marine nitrogen cycle. J. Plankton Res. 7 (4), 553–568.

Cherel, Y., Fontaine, C., Richard, P., Labat, J.-P., 2010. Isotopic niches and trophic levels of myctophid fishes and their predators in the Southern Ocean. Limnol. Oceanogr. 55 (1), 324–332. https://doi.org/10.4319/lo.2010.55.1.0324.

Danckwerts, D.K., Mcquaid, C.D., Jaeger, A., Mcgregor, G.K., Dwight, R., Le Corre, M., Jaquemet, S., 2014. Biomass consumption by breeding seabirds in the western Indian Ocean: indirect interactions with fisheries and implications for management. Mar. Sci. 71, 2589–2598. https://doi.org/10.1093/icesjms/fsu093.

De Forest, L., Drazen, J., 2009. The influence of a Hawaiian seamount on mesopelagic micronekton. Deep-Sea Res. Part I: Oceanogr. Res. Pap. 56 (2), 232–250. https://doi.org/10.1016/j.dsr.2008.09.007.

Ekau, W., Auel, H., Pörtner, H.-O., Gilbert, D., 2010. Impacts of hypoxia on the structure and processes in pelagic communities (zooplankton, macro-invertebrates and fish). Biogeosciences 7, 1669–1699. https://doi.org/10.5194/bg-7-1669-2010.

Fanelli, E., Papiol, V., Cartes, J.E., Rumolo, P., López-Pérez, C., 2013. Trophic webs of deep-sea megafauna on mainland and insular slopes of the NW Mediterranean: a comparison by stable isotope analysis. Mar. Ecol. Progr. Ser. 490, 199–221.

Gloeckler, K., Choy, C.A., Hannides, C.C.S., Close, H.G., Goetze, E., Popp, B.N., Drazen, J.C., 2017. Stable isotope analysis of micronekton around Hawaii reveals suspended particles are an important nutritional source in the lower mesopelagic and upper bathypelagic zones. Limnol. Oceanogr. https://doi.org/10.1002/lno.10762.

Guinet, C., Cherel, Y., Ridoux, V., Jouventin, P., 1996. Consumption of marine resources by seabirds and seals in Crozet and Kerguelen waters: changes in relation to consumer biomass 1962–85. Antarct. Sci. 8 (1), 23–30.

Hidaka, K., Kawaguchi, K., Murakami, M., Takahashi, M., 2001. Downward transport of organic carbon by diel migratory micronekton in the western equatorial pacific: its quantitative and qualitative importance. Deep-Sea Res. Part I: Oceanogr. Res. Pap. 48 (8), 1923–1939. https://doi.org/10.1016/S0967-0637(01)00003-6.

Hobson, K.A., Piatt, J.F., Pitocchelli, J., 1994. Using stable isotopes to determine seabird trophic relationships. J. Anim. Ecol. 63, 786–798.

Hu, V.J.H., 1978. Relationships between vertical migration and diet in four species of euphausiids. Limnol. Oceanogr. 23 (2), 296–306. https://doi.org/10.4319/lo.1978.23.2.0296.

Hudson, J.M., Steinberg, D.K., Sutton, T.T., Graves, J.E., Latour, R.J., 2014. Myctophid feeding ecology and carbon transport along the northern Mid-Atlantic Ridge. Deep-Sea Res. Part I 93, 104–116. https://doi.org/10.1016/j.dsr.2014.07.002.

Huggett, J.A., 2014. Mesoscale distribution and community composition of zooplankton in the Mozambique Channel. Deep Sea Res. Part II: Top. Stud. Oceanogr. 100, 119–135. https://doi.org/10.1016/j.dsr2.2013.10.021.

Hussey, N.E., MacNeil, M.A., McMeans, B.C., Olin, J.A., Dudley, S.F.J., Cliff, G., Wintner, S.P., Fennessy, S.T., Fisk, A.T., 2014. Rescaling the trophic structure of marine food webs. Ecol. Lett. 17, 239–250. https://doi.org/10.1111/ele.12226.

Jackson, A., Parnell, A.C., Inger, R., Bearhop, S., 2011. Comparing isotopic niche widths among and within communities: SIBER – Stable Isotope Bayesian Ellipses in R. J. Anim. Ecol. 80, 595–602. https://doi.org/10.1111/j.1365-2656.2011.01806.x.

Jaquemet, S., Ternon, J.F., Kaehler, S., Thiebot, J.B., Dyer, B., Bemanaja, E., Marteau, C., Le Corre, M., 2014. Contrasted structuring effects of mesoscale features on the seabird community in the Mozambique Channel. Deep-Sea Res. Part II: Top. Stud. Oceanogr. 100, 200–211. https://doi.org/10.1016/j.dsr2.2013.10.027.

Jena, B., Sahu, S., Avinash, K., Swain, D., 2013. Observation of oligotrophic gyre variability in the south Indian Ocean: environmental forcing and biological response. Deep-Sea Res. Part I 80, 1–10. https://doi.org/10.1016/j.dsr.2013.06.002.

Karl, D., Letelier, R., Tupas, L., Dore, J., Christian, J., Hebel, D., 1997. The role of nitrogen fixation in biogeochemical cycling in the subtropical North Pacific Ocean. Nature 388, 533–538.

Kikuchi, T., Omori, M., 1985. Vertical distribution and migration of oceanic shrimps at two locations off the Pacific coast of Japan. Deep-Sea Res. 32, 837–851.

Kolasinski, J., Kaehler, S., Jaquemet, S., 2012. Distribution and sources of particulate organic matter in a mesoscale eddy dipole in the Mozambique Channel (south-western Indian Ocean): insight from C and N stable isotopes. J. Mar. Syst. 96–97, 122–131. https://doi.org/10.1016/j.jmarsys.2012.02.015.

Lamont, T., Barlow, R.G., Morris, T., van den Berg, M.A., 2014. Characterisation of mesoscale features and phytoplankton variability in the Mozambique Channel. Deep-Sea Res. Part I 100, 94–105. https://doi.org/10.1016/j.dsr2.2013.10.019.

Lebourges-Dhaussy, A., Marchal, E., Menkes, C., Champalbert, G., Biessy, B., 2000. *Vinciguerria nimbaria* (micronekton), environment and tuna: their relationships in the Eastern Tropical Atlantic. Oceanol. Acta 23 (4), 515–528. https://doi.org/10.1016/S0399-1784(00)00137-7.

Lebourges-Dhaussy, A., Huggett, J., Ockhuis, S., Roudaut, G., Josse, E., Verheye, H., 2014. Zooplankton size and distribution within mesoscale structures in the Mozambique Channel: a comparative approach using the TAPS acoustic profiler, a multiple net sampler and ZooScan image analysis. Deep-Sea Res. Part II: Top. Stud. Oceanogr. 100, 136–152. https://doi.org/10.1016/j.dsr2.2013.10.022.

Lehodey, P., Andre, J.-M., Bertignac, M., Hampton, J., Stoens, A., Menkes, C., Memery, L., Grima, N., 1998. Predicting skipjack tuna forage distributions in the equatorial Pacific using a coupled dynamical bio-geochemical model. Fish. Oceanogr. 7 (3/4), 317–325. https://doi.org/10.1046/j.1365-2419.1998.00063.x.

Longhurst, A.R., Bedo, A.W., Harrison, W.G., Head, E.J.H., Sameoto, D.D., 1990. Vertical flux of respiratory carbon by oceanic diel migrant biota. Deep Sea Res. Part A Oceanogr. Res. Pap. 37 (4), 685–694.

Longhurst, A., 2007. The Indian Ocean-Indian South Subtropical Gyre Province (ISSG). In: Academic Press (Ed.), Ecological Geography of the Sea, 2nd ed. Elsevier, USA, pp. 285.

Lorrain, A., Graham, B.S., Popp, B.N., Allain, V., Olson, R.J., Hunt, B.P.V., Potier, M., Fry, B., Galvan-Magana, F., Menkes, C.E.R., Kaehler, S., Ménard, F., 2015. Nitrogen isotopic baselines and implications for estimating foraging habitat and trophic position of yellowfin tuna in the Indian and Pacific Oceans. Deep Sea Res. Part II: Top. Stud. Oceanogr. 113, 188–198. https://doi.org/10.1016/j.dsr2.2014.02.003.

Mapstone, G.M., 2014. Global diversity and review of Siphonophorae (Cnidaria: hydrozoa). PLoS One 9 (2), e87737. https://doi.org/10.1371/journal.pone.0087737.

Martínez Del Rio, C., Wolf, N., Carleton, S.A., Gannes, L.Z., 2009. Isotopic ecology ten years after a call for more laboratory experiments. Biol. Rev. 84 (1), 91–111. https://doi.org/10.1111/j.1469-185X.2008.00064.x.

McGillicuddy Jr, D.J., Robinson, A.R., Siegel, D.A., Jannasch, H.W., Johnson, R., Dickey, T.D., McNeil, J., Michaels, A.F., Knapk, A.H., 1998. Influence of mesoscale eddies on new production in the Sargasso Sea. Lett. Nat. 285, 263–266. https://doi.org/10.1038/28367.

Ménard, F., Potier, M., Jaquemet, S., Romanov, E., Sabatié, R., Cherel, Y., 2013. Pelagic cephalopods in the western Indian Ocean: new information from diets of top predators. Deep-Sea Res. Part II 95, 83–92.

Ménard, F., Benivary, H.D., Bodin, N., Coffineau, N., Le Loc'h, F., Mison, T., Richard, P., Potier, M., 2014. Stable isotope patterns in micronekton from the Mozambique Channel. Deep-Sea Res. Part II: Top. Stud. Oceanogr. 100, 153–163. https://doi.org/

10.1016/j.dsr2.2013.10.023.
Michener, R.H., Kaufman, L., 2007. Stable isotope ratios as tracers. In: Michener, Robert, Lajtha, Kate (Eds.), Stable Isotopes in Ecology and Environmental Science, Second Edition. https://doi.org/10.1002/9780470691854.ch9.
Minagawa, M., Wada, E., 1984. Stepwise enrichment of ^{15}N along food chains: further evidence and the relation between δ^{15}N and animal age. Geochim. Cosmochim. Acta 48, 1135–1140.
Mintenbeck, K., Jacob, U., Knust, R., Arntz, W.E., Brey, T., 2007. Depth-dependence in stable isotope ratio δ^{15}N of benthic POM consumers: the role of particle dynamics and organism trophic guild. Deep-Sea Res. Part I 54, 1015–1023. https://doi.org/10.1016/j.dsr.2007.03.005.
Mullin, M.M., Rau, G.H., Eppley, R.W., 1984. Stable nitrogen isotopes in zooplankton: some geographic and temporal variations in the North Pacific. Limnol. Oceanogr. 29 (6), 1267–1273. https://doi.org/10.4319/lo.1984.29.6.1267.
Oksanen, J., Blanchet, F.G., Friendly, M., Roeland, K., Legendre, P., McGlinn, D., Minchin, P.R., O'Hara, R.B., Simpson, G.L., Solymos, P., Stevens, M.H.H., Szoecs, E., Wagner, H., 2017. vegan: Community Ecology Package, R Package Version 2.4-5. . 〈https://CRAN.R-project.org/package=vegan.2017〉.
Olivar, M.P., Bernal, A., Molí, B., Peña, M., Balbín, R., Castellón, A., Miquel, J., Massutí, E., 2012. Vertical distribution, diversity and assemblages of mesopelagic fishes in the western Mediterranean. Deep Sea Res. Part I 62, 53–69.
Olivar, M.P., Hulley, P.A., Castellón, A., Emelianov, M., López, C., Tuset, V.M., Contreras, T., Molí, B., 2017. Mesopelagic fishes across the tropical and equatorial Atlantic: biogeographical and vertical patterns. Progr. Oceanogr. 151, 116–137.
Oschlies, A., Garcon, V., 1998. Eddy-induced enhancement of primary production in a model of the North Atlantic Ocean. Nature 394, 266–269. https://doi.org/10.1038/28373.
Otake, T., Nogami, K., Maruyaka, K., 1990. Possible food sources of eel leptocephali. La Mer 2 (8), 218–224.
Oudot, C., Morin, P., Baurand, F., Wafer, M., LeCorre, P., 1998. Northern and southern water masses in the equatorial Atlantic: distribution of nutrients on the WOCE A6 and A7 lines. Deep-Sea Res. Part I 45, 873–902.
Parry, M., 2008. Trophic variation with length in two ommastrephid squids, *Ommastrephes bartramii* and *Sthenoteuthis oualaniensis*. Mar. Biol. 153, 249–256. https://doi.org/10.1007/s00227-007-0800-3.
Pakhomov, E.A., Perissinotto, R., McQuaid, C.D., 1996. Prey composition and daily rations of myctophid fishes in the Southern Ocean. Mar. Ecol. Progr. Ser. 134, 1–14.
Polunin, N.V.C., Morales-Nin, B., Pawsey, W.E., Cartes, J.E., Pinnegar, J.K., Moranta, J., 2001. Feeding relationships in Mediterranean bathyal assemblages elucidated by stable nitrogen and carbon isotope data. Mar. Ecol. Progr. Ser. 220, 13–23. https://doi.org/10.3354/meps220013.
Post, D.M., 2002. Using stable isotopes to estimate trophic position: models, methods and assumptions. Ecology 83 (3), 703–718.
Potier, M., Marsac, F., Cherel, Y., Lucas, V., Sabatié, R., Maury, O., Ménard, F., 2007. Forage fauna in the diet of three large pelagic fishes (lancetfish, swordfish and yellowfin tuna) in the western equatorial Indian Ocean. Fish. Res. 83 (1), 60–72. https://doi.org/10.1016/j.fishres.2006.08.020.
Potier, M., Romanov, E., Cherel, Y., Sabatié, R., Zamorov, V., Ménard, F., 2008. Spatial distribution of *Cubiceps pauciradiatus* (Perciformes: nomeidae) in the tropical Indian Ocean and its importance in the diet of large pelagic fishes. Aquat. Living Resour. 21, 123–134. https://doi.org/10.1051/alr:2008026.
Potier, M., Bach, P., Ménard, F., Marsac, F., 2014. Influence of mesoscale features on micronekton and large pelagic fish communities in the Mozambique Channel. Deep Sea Res. Part II: Top. Stud. Oceanogr. 100, 184–199. https://doi.org/10.1016/j.dsr2.2013.10.026.
Pous, S., Lazure, P., André, G., Dumas, F., Halo, I., Penven, P., 2014. Circulation around la Réunion and Mauritius islands in the south-western Indian Ocean: a modeling perspective. J. Geophys. Res.: Oceans 119 (3), 1957–1976. https://doi.org/10.1002/2013JC009704.
Proud, R., Cox, M.J., Brierley, A.S., 2017. Biogeography of the Global Ocean's Mesopelagic Zone. Curr. Biol. 27, 113–119. https://doi.org/10.1016/j.cub.2016.11.003.
Quartly, G.D., Srokosz, M.A., 2004. Eddies in the southern Mozambique Channel. Deep-Sea Res. Part II: Top. Stud. Oceanogr. 51 (1–3), 69–83. https://doi.org/10.1016/j.dsr2.2003.03.001.
Reygondeau, G., Maury, O., Beaugrand, G., Fromentin, J.M., Fonteneau, A., Cury, P., 2012. Biogeography of tuna and billfish communities. J. Biogeogr. 39 (1), 114–129. https://doi.org/10.1111/j.1365-2699.2011.02582.x.
Robison, B.H., 1984. Herbivory by the myctophid fish *Ceratoscopelus warmingii*. Mar. Biol. 84, 119–123. https://doi.org/10.1007/BF00392995.
Rubenstein, D.R., Hobson, K.A., 2004. From birds to butterflies: animal movement patterns and stable isotopes. Trends Ecol. Evol. 19 (5), 256–263. https://doi.org/10.1016/j.tree.2004.03.017.
Schouten, M.W., De Ruijter, W.P.M., Van Leeuwen, P.J., Ridderinkhof, H., 2003. Eddies and variability in the Mozambique Channel. Deep-Sea Res. Part II: Top. Stud. Oceanogr. 50 (12–13), 1987–2003. https://doi.org/10.1016/S0967-0645(03)00042-0.
Seyboth, E., Botta, S., Mendes, C.R.B., Negrete, J., Dalla Rosa, L., Secchi, E.R., 2017. Isotopic evidence of the effect of warming on the northern Antarctic Peninsula ecosystem. Deep-Sea Res. Part I. https://doi.org/10.1016/j.dsr2.2017.12.020.
Stillwell, C.E., Kohler, N.E., 1985. Food and feeding ecology of the swordfish *Xiphias gladius* in the western North Atlantic Ocean with estimates of daily ration*. Mar. Ecol. Progr. Ser. 22 (1979430), 239–241. https://doi.org/10.3354/meps022239.
Stowasser, G., Atkinson, A., McGill, R.A.R., Phillips, R.A., Collins, M.A., Pond, D.W., 2012. Food web dynamics in the Scotia Sea in summer: a stable isotope study. Deep-Sea Res. Part II 59–60, 208–221. https://doi.org/10.1016/j.dsr2.2011.08.004.
Stramma, L., Lutjeharms, J.R.E., 1997. The flow field of the subtropical gyre of the South Indian Ocean. J. Geophys. Res. 102 (3), 5513–5530.
Sutton, T.T., Clark, M.R., Dunn, D.C., Halpin, P.N., Rogers, A.D., Guinotte, J., Bograd, S.J., Angel, M.V., Perez, J.A.A., Wishner, K., Haedrich, R.L., Lindsay, D.J., Drazen, J.C., Vereshchaka, A., Piatkowski, U., Morato, T., Blachowiak-Samolyk, K., Robison, B.H., Gjerde, K.M., Pierrot-Bults, A., Bernal, P., Reygondeau, G., Heino, M., 2017. A global biogeographic classification of the mesopelagic zone. Deep-Sea Res. Part I 126, 85–102. https://doi.org/10.1016/j.dsr.2017.05.006.
Tanaka, H., Ohshimo, S., Sassa, C., Aoki, I., 2007. Feeding habits of mesopelagic fishes off the coast of western Kyushu, Japan. In: Proceedings of the PICES 16th: Bio, p. 4200.
Tew-Kai, E., Marsac, F., 2009. Patterns of variability of sea surface chlorophyll in the Mozambique Channel: a quantitative approach. J. Mar. Syst. 77 (1–2), 77–88. https://doi.org/10.1016/j.jmarsys.2008.11.007.
Vanderklift, M.A., Ponsard, S., 2003. Sources of variation in consumer-diet δ^{15}N enrichment: a meta-analysis. Oecologia 136 (2), 169–182. https://doi.org/10.1007/s00442-003-1270-z.
von Harbou, L., 2009. Trophodynamics of Salps in the Atlantic Southern Ocean (Doctoral Dissertation). University of Bremen, Bremen, Germany. 〈http://nbn-resolving.de/urn:nbn:de:gbv:46-diss000119205〉.
Watanabe, H., Ohno, A., 1999. Diel vertical migration of myctophid fishes (Family Myctophidae) in the transitional waters of the western North Pacific. Fish. Oceanogr. 8 (2), 115–127.
Young, J.W., Hunt, B.P.V., Cook, T.R., Llopiz, J.K., Hazen, E.L., Pethybridge, H.R., Ceccarelli, D., Lorrain, A., Olson, R.J., Allain, V., Menkes, C., Patterson, T., Nicol, S., Lehodey, P., Kloser, R.J., Arrizabalaga, H., Choy, C.A., 2015. The trophodynamics of marine top predators: current knowledge, recent advances and challenges. Deep Sea Res. Part II: Top. Stud. Oceanogr. 113, 170–187. https://doi.org/10.1016/j.dsr2.2014.05.015.
Youngbluth, M.J., 1975. The vertical distribution and diel migration of euphausiids in the central waters of the eastern South Pacific. Deep-Sea Res. 22, 519–536. https://doi.org/10.1016/0011-7471(75)90033-9.
Zubkov, M.V., Quartly, G.D., 2003. Ultraplankton distribution in surface waters of the Mozambique Channel – flow cytometry and satellite imagery. Aquat. Microb. Ecol. 33 (2), 155–161.